Automating UbiFast for High-throughput and Multiplexed Ubiquitin Enrichment

Keith D. Rivera[1], Meagan E. Olive[1], Erik J. Bergstrom[1], Alissa J. Nelson[2], Kimberly A. Lee[2], Shankha Satpathy[1], Steven A. Carr[1]✉& Namrata D. Udeshi[1,✉]

[1]Broad Institute of MIT and Harvard, Cambridge, MA 02142, USA.
[2]Cell Signaling Technology, Danvers, MA 01923, USA

✉corresponding authors: udeshi@broadinstitute.org, scarr@broad.mit.edu

Abstract

Robust methods for deep-scale enrichment and site-specific identification of ubiquitylation sites is necessary for characterizing the myriad roles of protein ubiquitylation. To this end we previously developed UbiFast, a sensitive method for highly multiplexed ubiquitylation profiling where K-ε-GG peptides are enriched with anti-K-ε-GG antibody and labeled on-antibody with isobaric labeling reagents for sample multiplexing. Here, we present robotic automation of the UbiFast method using a magnetic bead-conjugated K-ε-GG antibody (mK-ε-GG) and a magnetic particle processor. We report the identification of ~20,000 ubiquitylation sites from a TMT10-plex with 500 µg input per sample processed in ~2 hours. Automation of the UbiFast method greatly increased the number of identified and quantified ubiquitylation sites, improved reproducibility and significantly reduced processing time. The workflow enables processing of up to 96 samples in a single day making it suitable to study ubiquitylation in large sample sets. Here we demonstrate the applicability of this method to profile small amounts of tissue using breast cancer patient-derived xenograft (PDX) tissue samples.

Introduction

Ubiquitylation is a highly-conserved protein post-translational modification regulating a wide variety of cellular functions including regulation of protein turnover through the ubiquitin-proteasome system [1]. The ubiquitylation process is regulated by E1 activating, E2 conjugating, E3 ligating enzymes together with deubiquitinases. Dysregulation of ubiquitylation enzymes and deubiquitinases can lead to aberrant activation or deactivation of pathways involved in many disease processes, notably cancer progression, neurodegeneration and innate and adaptive immune regulation[2]. Drugs targeting the ubiquitin system such as proteasome inhibitors have proven highly successful in the clinic. The development of additional therapeutics targeting this pathway are emerging but remain highly dependent on continued understanding of ubiquitination biology in disease[3–5].

Liquid chromatography-mass spectrometry (LC-MS/MS) is the leading method for unbiased analysis of protein modifications, including protein ubiquitylation. Analysis of ubiquitylated proteins is typically carried out by first using trypsin to generate peptides suitable for LC-MS/MS analysis. Trypsin cleaves proteins at the carboxyl side of lysine (Lys) and arginine (Arg). When ubiquitin is attached to a substrate protein, trypsin digestion leaves a glycine-glycine (GG) remnant on the side chain of Lys residues of tryptic peptides which were formerly ubiquitylated. Antibodies that recognize this di-glycl remnant (K-ε-GG) are used to enrich ubiquitylated (Ub) peptides for analysis by liquid-chromatography- tandem mass spectrometry (LC-MS/MS)[6–9].

Isobaric chemical tags such as the Tandem Mass Tag (TMT) system are commonly used to compare up to 16 samples within a single experiment and provide

precise relative quantitation of peptides and proteins[10–12]. A major limitation of integrating TMT quantitation and ubiquitylation profiling with K-ε-GG antibodies is that these antibodies no longer recognize and enrich peptides when the N-terminus of the di-glycyl remnant is derivatized with TMT. To overcome this limitation, we recently developed the UbiFast method for highly sensitive and multiplexed analysis of ubiquitylation sites from cells or tissue[13]. The UbiFast method employs an anti-K-ε-GG antibody for enrichment of K-ε-GG peptides followed by on-antibody TMT labeling. Specifically, K-ε-GG peptides are labeled with TMT reagents while still bound to the anti-K-ε-GG antibody which allows the NHS-ester group of the TMT reagent to react with the peptide N-terminal amine group and the ε-amine groups of lysine residues, but not the primary amine of the di-glycyl remnant. In this way, TMT-labeled K-ε-GG peptides from each sample are combined, eluted from the antibody, and analyzed by LC-MS/MS. The UbiFast approach eliminates cell culture restrictions, greatly reducing the amount of input material required when using SILAC-based experiments[6,7,14–20] and improves Ub-peptide recovery and analysis time compared to in-solution TMT labeling strategies [21]. The sensitivity of the UbiFast method makes it suitable for studies in primary tissue samples.

Although the UbiFast method is highly effective for deep-scale LC-MS/MS analysis of ubiquitylated peptides, the throughput is limited because all workflow steps are manually executed, making the procedure laborious. Additionally, an initial cross-linking step is necessary to covalently couple the antibody to agarose beads, which prevents contamination of antibody in enriched samples [7]. Further, slight variations during the K-ε-GG peptide enrichment step can result in an increased variability across replicates within a given TMT experiment.

To improve the UbiFast method, here we evaluate and optimize use of a commercially available anti-K-ε-GG antibody supplied irreversibly coupled to magnetic beads (HSmag anti-K-ε-GG). Additionally, we demonstrate that HSmag anti-K-ε-GG antibody enables automation of the UbiFast method on a magnetic bead processor greatly increasing sample processing throughput while maintaining low variation across experimental replicates (Figure 1). We also show that the automated UbiFast method can be easily scaled to process multiple 10-plex TMT experiments in just a few hours. The automated UbiFast method was benchmarked against the previously published, manually executed UbiFast method for profiling patient-derived breast cancer xenograft tissue.

Results

Comparison of magnetic- and agarose-bead antibody reagents for manual enrichment of K-ε-GG peptides

The PTMScan® HS Ubiquitin/SUMO Remnant Motif (K-ε-GG) Kit (#59322) contains the same monoclonal antibody as the original PTMScan Ubiquitin Remnant (K-ε-GG Kit) (#5562), with the key difference that the new kit contains magnetic beads instead of agarose and bind and wash buffers have been optimized to maximize sensitivity and specificity of K-ε-GG peptide enrichment. The antibody is coupled to the beads using chemistry that does not affect the epitope binding regions. Since this HSmag anti-K-ε-GG formulation does not require an initial chemical cross-linking step to covalently couple the antibody to affinity beads, 1-2 days of procedural time are saved[7,21,22]. The magnetic bead formulation also provides the means to transfer ubiquitin

enrichment protocols to a magnetic particle processor for automating and increasing the throughput of sample handling steps.

To characterize the performance of HSmag anti-K-ε-GG, the enrichment of K-ε-GG peptides was directly compared to enrichment with agarose-bead anti-K-ε-GG antibody in a label-free manner by LC-MS/MS. Enrichment of K-ε-GG peptides was completed in triplicate from 500 µg of tryptic peptides derived from Jurkat cells using 5 µl and 10 µl of HSmag anti-K-ε-GG slurry vs. 8 µl of agarose-bead anti-K-ε-GG antibody and enriched peptides were analyzed by LC-MS/MS (Supplemental Figure 1 and Supplemental Data 1). Previous work has shown 8 µl anti-K-ε-GG agarose-bead reagent to be optimal for enrichment of K-ε-GG peptides[23]. An average of 8662 K-ε-GG PSMs were identified with 5 µl of HSmag anti-K-ε-GG, 9284 K-ε-GG PSMs were identified with 10 µl of HSmag anti-K-ε-GG and 6643 K-ε-GG PSMs were identified with 8 µl anti-K-ε-GG agarose-bead antibody. Using 5 µl or 10 µl of HSmag anti-K-ε-GG improved recovery of K-ε-GG PSMs compared to 8 µl anti-K-ε-GG agarose-bead antibody by 30% and 39%, respectively. The relative yield, or the percentage of K-ε-GG PSMs identified relative to the total number of PSMs identified in the sample, was 51% with 5 µl of HSmag anti-K-ε-GG, 57% with 10 µl of HSmag anti-K-ε-GG and 32% with 8 µl anti-K-ε-GG agarose-bead antibody. These results show that HSmag anti-K-ε-GG beads outperform anti-K-ε-GG agarose-bead antibody reagent for the enrichment of K-ε-GG peptides using as little as 5 µl of magnetic beads. Although 10 µl of HS mag anti-K-ε-GG beads minimized variability, it provided only a relatively small increase in the number of identified K-ε-GG PSMs vs. the use of 5 µl of HSmag anti-K-ε-GG slurry, indicating that the lower amount of beads is efficient and cost effective.

Evaluation of on-antibody TMT labeling using HSmag anti-K-ε-GG

The UbiFast method utilizes on-antibody TMT labeling for isobaric labeling experiments[13]. To evaluate the performance of on-antibody TMT labeling using HSmag anti-K-ε-GG antibody, Jurkat peptides (500 µg in triplicate) were enriched using HSmag anti-K-ε-GG or agarose-bead anti-K-ε-GG antibody and labeled with TMT reagent as previously described[13] (Supplemental Data 2). For this evaluation, a single channel of TMT reagent was used to label each replicate. We identified an average of 8008 and 5289 K-ε-GG PSMs with 5 µL magnetic and 8µL agarose-bead antibody reagent, respectively (Supplemental Fig 1b).

To analyze the efficiency of TMT labeling we evaluated the number of K-ε-GG PSMs fully TMT labeled, partially TMT labeled and unlabeled. A peptide is considered fully labeled if the N-terminal amine group (-NH_2) and the ε-amino group on lysines (if present) have reacted with the TMT reagent. Partially labeled PSMs have one amine group that has reacted with TMT and at least one amine group that has not reacted with the TMT reagent. For the agarose bead experiments, 91% of the K-ε-GG PSMs were fully labeled and 5% were partially labeled. For the magnetic bead experiments, 91% of the K-ε-GG PSMs were fully labeled and 5% were partially labeled (Supplemental Fig 1c). The overlap of K-ε-GG sites identified using HSmag anti-K-ε-GG and anti-K-ε-GG antibody was >52% (Supplemental Figure 1d). Each method also identified a subset of distinct Ub sites. These results demonstrate that on-antibody TMT labeling works effectively with HSmag anti-K-ε-GG and HSmag anti-K-ε-GG outperforms anti-K-ε-GG antibody for identifying K-ε-GG peptides following enrichment and on-antibody TMT labeling.

Optimization of automated workflow for the UbiFast method

To increase the throughput and reproducibility of the UbiFast method, we sought to reduce the number of manual sample processing steps in the method by automating the HSmag anti-K-ε-GG washing and on-antibody TMT labeling steps using the KingFisher Flex (KF), a magnetic bead processor capable of processing 96-well plates. The KF operates by using magnetic rods to collect magnetic beads from a 96-well plate and transfer them into another 96-well plate. Following offline K-ε-GG peptide capture in a 96 well plate, the plate was loaded onto the KF where antibody beads were washed and K-ε-GG peptides labeled with TMT reagent while still on HSmag anti-K-ε-GG beads (Supplemental Figure 2).

First, we evaluated how efficiently HSmag anti-K-ε-GG transfer from one 96-well plate to a second 96-well plate on the KF. Previous work showed that adding low concentrations of CHAPS to buffers prevents magnetic beads from sticking to the plates and being lost during KF processing steps [24]. We compared automated UbiFast with and without addition of 0.01% CHAPS to wash buffers and found that CHAPS significantly improves the automated protocol, identifying 1.9-fold more K-ε-GG peptides compared to no CHAPS addition (3329 vs 1752 K-ε-GG PSMs) (Supplemental Figure 3a, Supplemental Data 3). Omitting CHAPS from wash buffers clearly resulted in residual HSmag anti-K-ε-GG beads being left in the plates after the completion of the KF run. These experiments confirmed that CHAPS improves the movement of magnetic beads in this protocol, increasing the number of K-ε-GG PSMs by 89% and decreasing variability due to loss of beads and should be added to all buffers used on the KF platform.

We next tested if capture of K-ε-GG peptides with HSmag anti-K-ε-GG could be completed on the KF. In the manual protocol, the enrichment step is complete at 4□ with end-over-end rotation[7]. The KF does not have a cooling unit and cannot rotate plates end-over-end. Therefore we sought to confirm whether the enrichment step should be performed offline as is done in the manual protocol or on the KF at RT with mixing. To evaluate the capture step, two 96-well KF plates were prepared, each with three wells containing 500 µg Jurkat peptides and the HSmag anti-K-ε-GG. One 96-well plate was rotated end-over-end in a cold room at 4°C and the other plate was incubated on the KF at room temperature with mixing set to 'medium' (Supplemental Figure 3b, Supplemental Data 4). A large drop in PSMs was observed when the incubation was performed at RT on the KingFisher, identifying 3308 K-ε-GG PSMs compared to 6215 K-ε-GG PSMs with end-over-end rotation at 4°C. These results indicate that offline end-over-end rotation at 4°C is preferable for binding of K-ε-GG peptides to the HSmag anti-K-ε-GG. Performing this step offline will not add any additional time or labor since the samples and beads are already in the 96-well plate, however, future studies could explore placing the KingFisher in a cold room at 4°C.

Next we determined the optimal HSmag anti-K-ε-GG amount for K-ε-GG peptide enrichment on the KF. Previous work showed that decreasing the amount of agarose-bead anti-K-ε-GG antibody increased the relative yield and overall recovery of K-ε-GG peptides[7]. Given the previous findings, we titrated the amount of HSmag anti-K-ε-GG to determine which bead volume would produce the highest overall number and the highest relative yield of K-ε-GG peptides. We performed quintuplicate enrichments using 5 µL, 10 µL and 20 µL of HSmag anti-K-ε-GG and compared the overall number of K-ε-GG PSMs

and relative yield (Supplemental Figure 3c, Supplemental Data 5). The number of identified K-ε-GG PSMs was 6519, 5261 and 4540 for 5, 10 and 20 µL of HSmag anti-K-ε-GG, respectively. The relative yield of K-ε-GG PSMs was 29%, 23% and 20% for 5, 10 and 20 µL of HSmag anti-K-ε-GG, respectively. Enrichment with 5 µL HSmag anti-K-ε-GG provided the best overall number of K-ε-GG PSMs and relative yield of K-ε-GG PSMs.

We noted that the relative yield of K-ε-GG PSMs to total PSMs was much lower for HSmag anti-K-ε-GG processing on the KF relative to manual processing (29% vs 51%). We hypothesized that the decrease in relative yield of K-ε-GG peptides could be due to insufficient bead washing because the volume of each wash step was reduced from 1 mL in the manual protocol to 250 µL on the KF to accommodate the maximum volume of the 96-well plate. To reduce the number of non-K-ε-GG peptides resulting from automated processing, 50% ACN was added to the wash buffer to increase stringency. To evaluate the utility of ACN addition to the wash buffer, we performed a label-free experiment where K-ε-GG peptides were enriched from 500 µg Jurkat peptides where bead washing was completed with or without 50% ACN added to the HS IAP Wash Buffer (Supplemental Figure 3d, Supplemental Data 6). Addition of 50% ACN to the washing buffer increased both the relative yield of K-ε-GG peptides and the absolute number of identified K-ε-GG peptides. An average of 7210 K-ε-GG PSMs with 57% relative yield and 5694 K-ε-GG PSMs with 29% relative yield were identified with and without 50% ACN added to the wash buffer, respectively. Taken together, we find that use of 5 µL of HSmag anti-K-ε-GG bead slurry and inclusion of 0.01% CHAPS and 50% ACN in wash buffers provides the best performance of the UbiFast method on the KF.

Manual vs. automated TMT 10-plex experiment

The Ubifast method is designed to be used with multiplexed samples[13]. To evaluate the performance of the automated UbiFast workflow, we carried out a head-to-head comparison using HSmag anti-K-ε-GG where both automated and manual UbiFast methods were used to analyze 10 process replicates of peptides from Jurkat cells, with 500 ug peptide input per replicate using a different TMT10 reagent for each replicate. Due to the additional time it takes to prepare and aliquot TMT reagents in a 96-well plate for multiplexed experiments, we performed two independent automated TMT10 UbiFast experiments comparing 10 minutes and 20 minutes on-antibody TMT labeling time to determine if a longer TMT labeling time is needed due to reagent hydrolysis during preparation steps (Figure 2a). For manual and automated experiments, we assessed the efficiency of TMT labeling, relative yield of K-ε-GG peptides and the variability between differentially labeled TMT channels (Figure 2b, 2c, 2d, Supplemental Data 7).

Using the manual UbiFast protocol, we identified 16,141 distinct K-ε-GG peptides with 97% of peptides being labeled with TMT and a relative yield of 75%. The automated UbiFast experiment identified 21,468 with 88% relative yield and 21,601 distinct K-ε-GG peptides with 87% relative yield using 10 and 20 minutes of on-antibody TMT labeling time, respectively. Increasing on-antibody TMT labeling time from 10 min to 20 min increased the TMT labeling efficiency from 95% to 97%. The reproducibility of automated UbiFast experiments was higher than manual UbiFast, with median coefficients of variation across process replicates of 20%, 19%, 25% for automated UbiFast 10min, automated UbiFast 20 min, manual UbiFast, respectively. These data indicate the

automated platform washes enriched K-ε-GG peptides and performs on-antibody TMT labeling with high reproducibility, eliminating the need for manual processing.

Performing multiple experiments in parallel using the automated UbiFast method

Automating the UbiFast method reduces the hands-on time for processing a single multiplexed TMT experiment, but the greatest impact would be in the ability to scale the number of multiplexed TMT experiments that could be processed simultaneously. To evaluate the effects of processing multiple TMT experiments, we designed an experiment in which 4 x TMT10 experiments were processed in parallel (Figure 3a). Briefly, a batch of peptides digested with trypsin from A375 cells were aliquoted into 40 x 500 µg aliquots. The 40 aliquots were split into 4 groups of 10 and processed on the KF as described above with each group of 10 aliquots processed as separate TMT10 experiments. To assess performance across all 4 experiments, we evaluated the number of distinct K-ε-GG peptides, the coefficient of variation for each experiment and the labeling efficiency (Figure 3b, 3c, 3d, Supplemental Data 8). We identified 17,718, 16,704, 17,668 and 16,862 distinct K-ε-GG peptides in experiments 1 through 4, respectively. The median coefficient of variation for each plex was 20.8, 19.8, 21.2 and 20.8 and the percentage of fully labeled K-ε-GG PSMs was 95%-96% for all 4 plexes. These results indicate that the automated UbiFast protocol enables multiple multiplexed TMT experiments to be processed simultaneously with high reproducibility, saving up to 2 hours of laboratory time for each additional TMT experiment.

Application of automated UbiFast with HSmag anti-K-ε-GG to analysis of tumor samples

Tumor tissues of two breast cancer patient-derived xenograft (PDX) models, basal subtype (WHIM2) and luminal subtype (WHIM16) have been extensively characterized in the proteogenomic space, having been shown to harbor subtype-specific signatures[13,25,26]. To evaluate our automated UbiFast method for profiling ubiquitylomes of small amounts of tumor tissue, we applied the workflow to enrich ubiquitylated peptides from five replicates each of WHIM2 and WHIM16 using 0.5 mg of peptide per sample in a TMT10-plex experiment (Figure 4a). The correlation of replicates within the automated UbiFast dataset employing HSmag anti-K-ε-GG beads was high, with median Pearson correlations of 0.76 and 0.73 for basal and luminal subtypes, respectively (Figure 4b, Supplemental Data 9). In total, 14,211 distinct K-ε-GG peptides were identified and quantified using this method. Ubiquitylation data was compared to previously published results acquired on the sample PDX models, but employing UbiFast in a manual mode using agarose K-ε-GG antibody to evaluate the overlap of K-ε-GG sites and conservation of canonical biological differences between basal and luminal breast cancer models. Among these identified K-ε-GG sites, we see a high degree of overlap at the site level (61%) between datasets (Figure 4c). To assess whether biological changes were conserved across UbiFast workflows, we performed gene set enrichment analysis (GSEA) on both datasets using the GO Biological Process Molecular Signature Database[27,28]. Gene Sets which were significantly changing in both datasets are shown in Figure 4d with the top 5 gene sets enriched in the luminal and basal subtypes from the Udeshi et al. 2020 study highlighted. It is clear that the gene sets which were significantly

enriched with the automated method show the same trends as those enriched by Udeshi et al. 2020.

Discussion

Here we present an automated UbiFast workflow using magnetic-bead K-ε-GG antibody and a robotic magnetic particle processor with a 96 well plate format to increase sample analysis throughput of the UbiFast method while decreasing labor required and chances for human error (Figure 1). Removing the need for a highly trained person to perform these enrichments should make ubiquitylation site profiling accessible to more laboratories. Using the manual implementation of the UbiFast method, it takes more than 1 day of processing time to prepare 10 samples (1 x 10-plex experiment) for injection on the mass spectrometer because the antibody must first be cross-linked to agarose beads followed by quality control[26]. Magnetic HSmag anti-K-ε-GG supplied in the PTMScan® HS Ubiquitin/SUMO Remnant Motif (K-ε-GG) kit are provided with the antibody already linked to the magnetic beads and do not require additional cross-linking, simplifying the method and reducing the total processing time to 3 hours per 1 x 10-plex experiment. Importantly, the magnetic HSmag anti-K-ε-GG reagent identified more Ub-peptides with greater reproducibility than the agarose anti-K-ε-GG reagent in TMT experiments. Automation of the UbiFast method on the KF reduces sample processing time per plex from 3 hours to 2 hours and allows for parallel processing of up to 9 x TMT10-plex experiments. Future efforts will be aimed at extending to higher-plex isobaric labeling methods such as TMTPro (Thermo Fisher), enabling 6 x 16-plex experiments to be processed in parallel. The KF platform may be used to automate the enrichment of other

PTMs, such as phosphorylated tyrosine and acetylated lysines as magnetic bead reagents become available in the future.

Figure Legends

Figure 1. Comparison of methods for on-antibody labeling of K-ε-GG peptides with isobaric reagents. a Workflow of on-antibody labeling of K-ε-GG peptides with isobaric reagents using the UbiFast method. b Manual UbiFast workflow for processing a TMT10 experiment. c Automated workflow of processing samples for a TMT10 experiment using 96-well plates and a KingFisher Flex instrument.

Figure 2. Analysis of K-ε-GG peptide enrichment in a 10-plex format using automation vs. manual workflows. a Experimental design of parallel 10-plex ubiquitin enrichment experiments using TMT10 reagents for on-antibody TMT labeling. **b** Stacked bar plots show the percentage of fully, partially and unlabeled K-ε-GG PSM **c** Bar plots of K-ε-GG (green) and non K-ε-GG (blue) distinct peptides identified in each experiment. **d** Violin plots show the distribution of CV's between differentially labeled TMT channels for each experiment with the inner box and whisker plots showing the median and interquartile range.

Figure 3. Parallel processing of 4 x TMT10 experiments using the automated UbiFast method. a Schematic of experimental workflow for processing multiple experiments in parallel. b Stacked bar plots show the percentage of fully, partially and unlabeled K-ε-GG PSMs. c Bar plots of K-ε-GG (green) and non K-ε-GG (blue) distinct

peptides identified in each experiment. d Violin plots show the distribution of CV's between differentially labeled TMT channels for each experiment with the inner box and whisker plots showing the median and interquartile range

Figure 4. Comparison of the ubiquitylomes identified from our automated workflow vs manually workflow[13]. a Schematic diagram showing experimental design and process used to enrich K-ε-GG modified peptides from the Luminal and Basal breast cancer PDX models. b Venn Diagram showing overlap of K-ε-GG sites identified in each dataset. c Box of whisker plots of Pearson correlation between replicates of Basal and Luminal PDX models for each dataset. d Heatmap of all genesets present in both the Udeshi et al dataset (left) and the current, automated dataset (right) with the top 5 most enriched gene sets in the Udeshi et al dataset highlighted.

Supplemental Figures

Supplemental Figure 1. Comparison of K-ε-GG peptide enrichments with antibody coupled to either agarose or magnetic beads. a Bar plots show identification of K-ε-GG and non K-ε-GG PSMs for label free enrichments with agarose and magnetic beads (n=3). b Bar plots show the identification of of K-ε-GG and non K-ε-GG PSMs from enrichments with on-antibody labeling with single channel TMT (n=3). c Stacked bar plots show the percentage of fully labeled, partially labeled, unlabeled and sequences with no capacity for labeling. d Venn diagram showing overlap of peptides identified with agarose and magnetic beads e Table showing all raw values, including enrichment specificity for previously described experiments.

Supplemental Figure 2. Setup and processing steps for using the KingFisher Flex to automate ubiquitin enrichment. a Plate contents for each of the 8 96-well KF plates. b Overview of each step in the automated ubiquitin enrichment process.

Supplemental Figure 3. Optimization of bead amounts and washing buffer for K-ε-GG enrichments using the KingFisher Flex instrument. a Bar plots showing identification of K-ε-GG PSMs when 0.01% CHAPS is either absent or present from buffers used on the KingFisher platform. b Bar plots showing identifications of K-ε-GG PSMs from enrichments where the binding of K-ε-GG peptides occurred for 1 hour on the KF robot at RT or 1 hour with end-over-end mixing at 4 °C. **c** Bar plots show identification of K-ε-GG and non K-ε-GG PSM for enrichments using varying amounts of beads (n=5). **d** Bar plots show the identification of K-ε-GG and non K-ε-GG PSM from enrichments with either HS IAP Wash Buffer or HS IAP Wash Buffer diluted 1:1 with ACN.

Acknowledgements

This work was supported by the National Cancer Institute (NCI) grants U24CA210986, U01CA214125, and U24CA210979 to S.A.C., Swiss National Science Foundation (SNF) Sinergia grant CRSII5_186405 to S.A.C., Dr. Miriam and Sheldon G. Adelson Medical Research Foundation to S.A.C. and N.D.U. and by a SPARC Award to N.D.U. from the Broad Institute of MIT & Harvard (#800373)

Authors contribution

K.D.R., M.E.O., S.A.C. and N.D.U. conceived the study; K.D.R., M.E.O., and E.J.B. performed experiments. K.D.R., M.E.O., E.J.B., A.J.N., K.A.L., S.S., S.A.C. and N.D.U. contributed to experimental design, data analysis, and data interpretation. K.D.R., M.E.O., S.A.C. and N.D.U. generated figures and wrote the manuscript with input from all authors.

References

1. Hershko, A. & Ciechanover, A. The ubiquitin system. *Annu. Rev. Biochem.* **67**, 425–479 (1998).
2. Celebi, G., Kesim, H., Ozer, E. & Kutlu, O. The Effect of Dysfunctional Ubiquitin Enzymes in the Pathogenesis of Most Common Diseases. *Int. J. Mol. Sci.* **21**, (2020).
3. Kortuem, K. M. & Stewart, A. K. Carfilzomib. *Blood* **121**, 893–897 (2013).
4. Hideshima, T. *et al.* The proteasome inhibitor PS-341 inhibits growth, induces apoptosis, and overcomes drug resistance in human multiple myeloma cells. *Cancer Res.* **61**, 3071–3076 (2001).
5. Schapira, M., Calabrese, M. F., Bullock, A. N. & Crews, C. M. Targeted protein degradation: expanding the toolbox. *Nat. Rev. Drug Discov.* **18**, 949–963 (2019).
6. Kim, W. *et al.* Systematic and Quantitative Assessment of the Ubiquitin-Modified Proteome. *Mol. Cell* **44**, 325–340 (2011).
7. Udeshi, N. D., Mertins, P., Svinkina, T. & Carr, S. A. Large-scale identification of ubiquitination sites by mass spectrometry. *Nat. Protoc.* **8**, 1950–1960 (2013).
8. Na, C. H. *et al.* Synaptic Protein Ubiquitination in Rat Brain Revealed by Antibody-based Ubiquitome Analysis. *J. Proteome Res.* **11**, 4722–4732 (2012).

9. Xu, G., Paige, J. S. & Jaffrey, S. R. Global analysis of lysine ubiquitination by ubiquitin remnant immunoaffinity profiling. *Nat. Biotechnol.* **28**, 868–873 (2010).
10. Thompson, A. *et al.* Tandem Mass Tags: A Novel Quantification Strategy for Comparative Analysis of Complex Protein Mixtures by MS/MS. *Anal. Chem.* **75**, 1895–1904 (2003).
11. Thompson, A. *et al.* TMTpro: Design, Synthesis, and Initial Evaluation of a Proline-Based Isobaric 16-Plex Tandem Mass Tag Reagent Set. *Anal. Chem.* **91**, 15941–15950 (2019).
12. Li, J. *et al.* TMTpro reagents: a set of isobaric labeling mass tags enables simultaneous proteome-wide measurements across 16 samples. *Nat. Methods* **17**, 399–404 (2020).
13. Udeshi, N. D. *et al.* Rapid and deep-scale ubiquitylation profiling for biology and translational research. *Nat. Commun.* **11**, (2020).
14. Emanuele, M. J. *et al.* Global Identification of Modular Cullin-RING Ligase Substrates. *Cell* **147**, 459–474 (2011).
15. Gendron, J. M. *et al.* Using the Ubiquitin-modified Proteome to Monitor Distinct and Spatially Restricted Protein Homeostasis Dysfunction. *Mol. Cell. Proteomics* **15**, 2576–2593 (2016).
16. Kronke, J. *et al.* Lenalidomide Causes Selective Degradation of IKZF1 and IKZF3 in Multiple Myeloma Cells. *Science* **343**, 301–305 (2014).
17. Povlsen, L. K. *et al.* Systems-wide analysis of ubiquitylation dynamics reveals a key role for PAF15 ubiquitylation in DNA-damage bypass. *Nat. Cell Biol.* **14**, 1089–1098 (2012).
18. Sarraf, S. A. *et al.* Landscape of the PARKIN-dependent ubiquitylome in response to mitochondrial depolarization. *Nature* **496**, 372–376 (2013).
19. Satpathy, S. *et al.* Systems□wide analysis of BCR signalosomes and downstream phosphorylation and ubiquitylation. *Mol. Syst. Biol.* **11**, 810 (2015).
20. Wagner, S. A., Satpathy, S., Beli, P. & Choudhary, C. SPATA2 links CYLD to the TNF□α receptor signaling complex and modulates the receptor signaling outcomes. *EMBO J.* **35**, 1868–1884 (2016).

21. Rose, C. M. *et al.* Highly Multiplexed Quantitative Mass Spectrometry Analysis of Ubiquitylomes. *Cell Systems* **3**, 395–403.e4 (2016).
22. Hansen, F. M. *et al.* Data-independent acquisition method for ubiquitinome analysis reveals regulation of circadian biology. *Nat. Commun.* **12**, 1–13 (2021).
23. Udeshi, N. D. *et al.* Refined preparation and use of anti-diglycine remnant (K-ε-GG) antibody enables routine quantification of 10,000s of ubiquitination sites in single proteomics experiments. *Mol. Cell. Proteomics* **12**, 825–831 (2013).
24. Kuhn, E. *et al.* Interlaboratory evaluation of automated, multiplexed peptide immunoaffinity enrichment coupled to multiple reaction monitoring mass spectrometry for quantifying proteins in plasma. *Mol. Cell. Proteomics* **11**, M111 013854 (2012).
25. Li, S. *et al.* Endocrine-Therapy-Resistant ESR1 Variants Revealed by Genomic Characterization of Breast-Cancer-Derived Xenografts. *Cell Rep.* **4**, 1116–1130 (2013).
26. Mertins, P. *et al.* Reproducible workflow for multiplexed deep-scale proteome and phosphoproteome analysis of tumor tissues by liquid chromatography–mass spectrometry. *Nat. Protoc.* **13**, 1632–1661 (2018).
27. Subramanian, A. *et al.* Gene set enrichment analysis: A knowledge-based approach for interpreting genome-wide expression profiles. *Proceedings of the National Academy of Sciences* **102**, 15545–15550 (2005).
28. Mootha, V. K. *et al.* PGC-1α-responsive genes involved in oxidative phosphorylation are coordinately downregulated in human diabetes. *Nat. Genet.* **34**, 267–273 (2003).
29. Shadforth, I. P., Dunkley, T. P. J., Lilley, K. S. & Bessant, C. i-Tracker: For quantitative proteomics using iTRAQ™. *BMC Genomics* **6**, 1–6 (2005).
30. Benjamini, Y. & Hochberg, Y. Controlling the false discovery rate: A practical and powerful approach to multiple testing. *J. R. Stat. Soc.* **57**, 289–300 (1995).

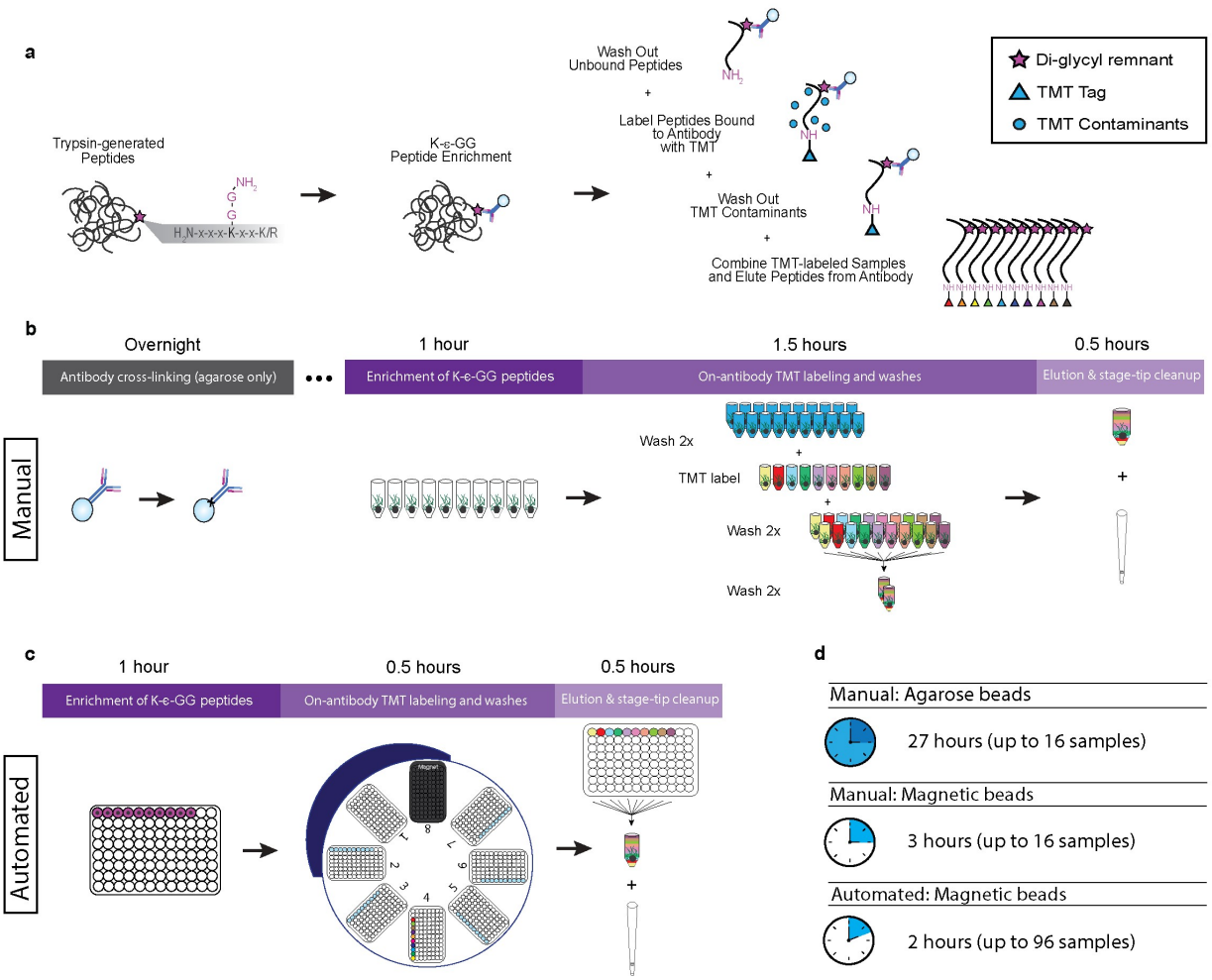

Figure 1

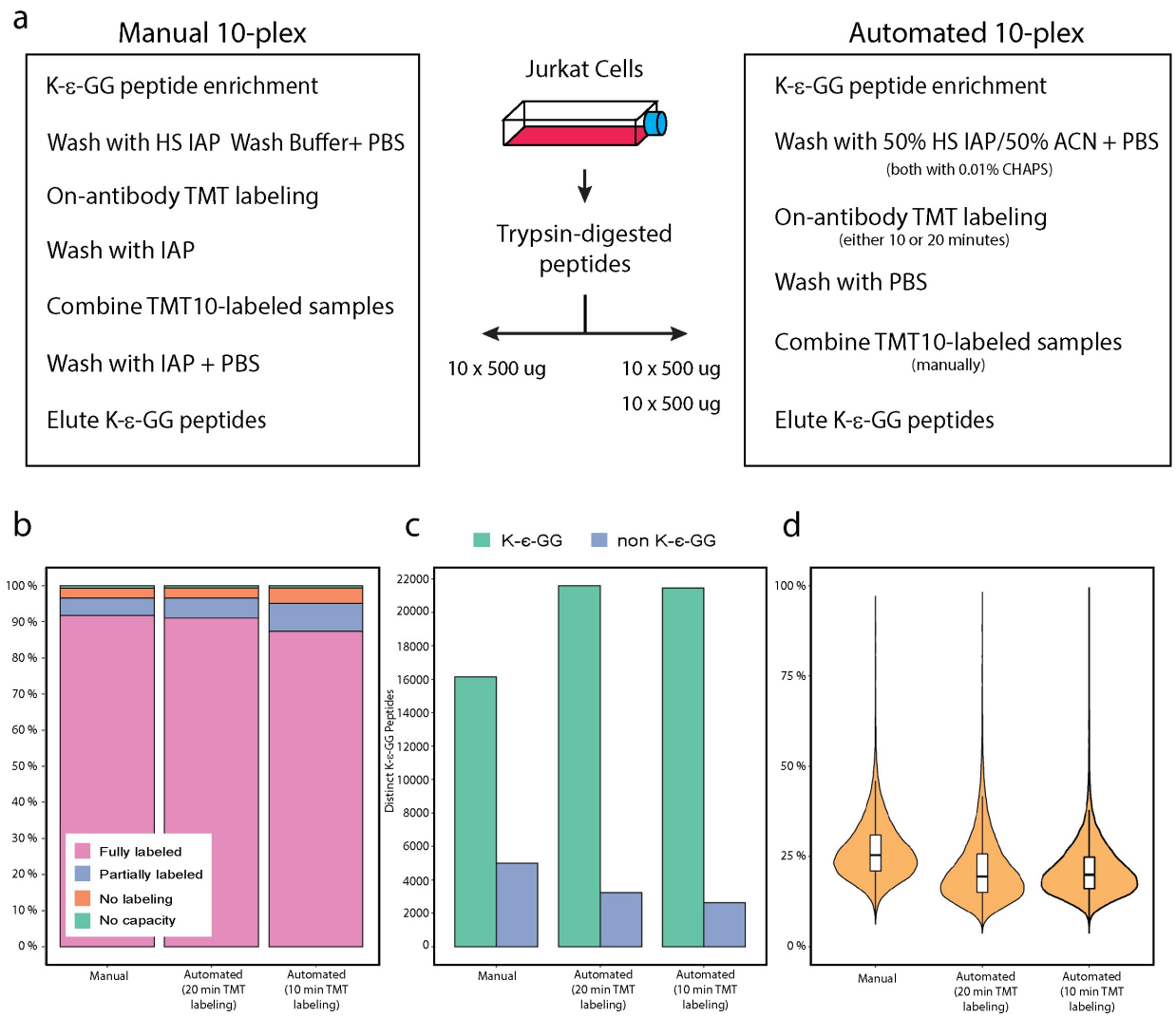

Figure 2

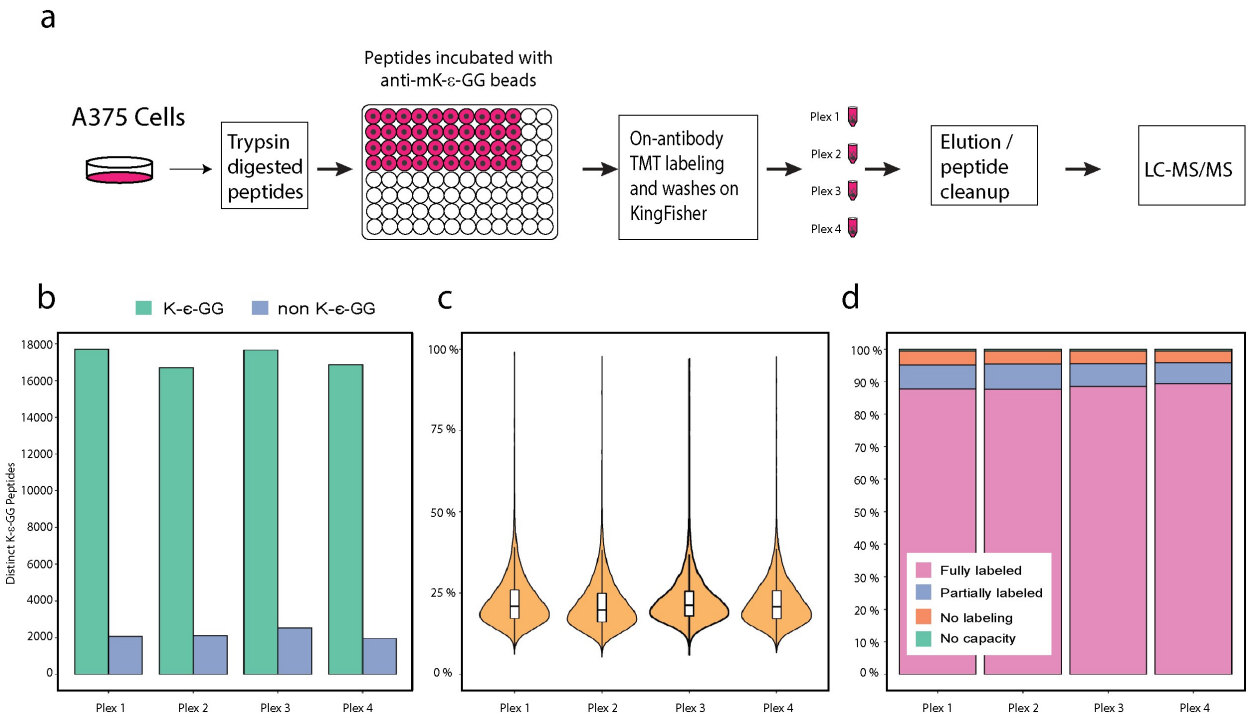

Figure 3

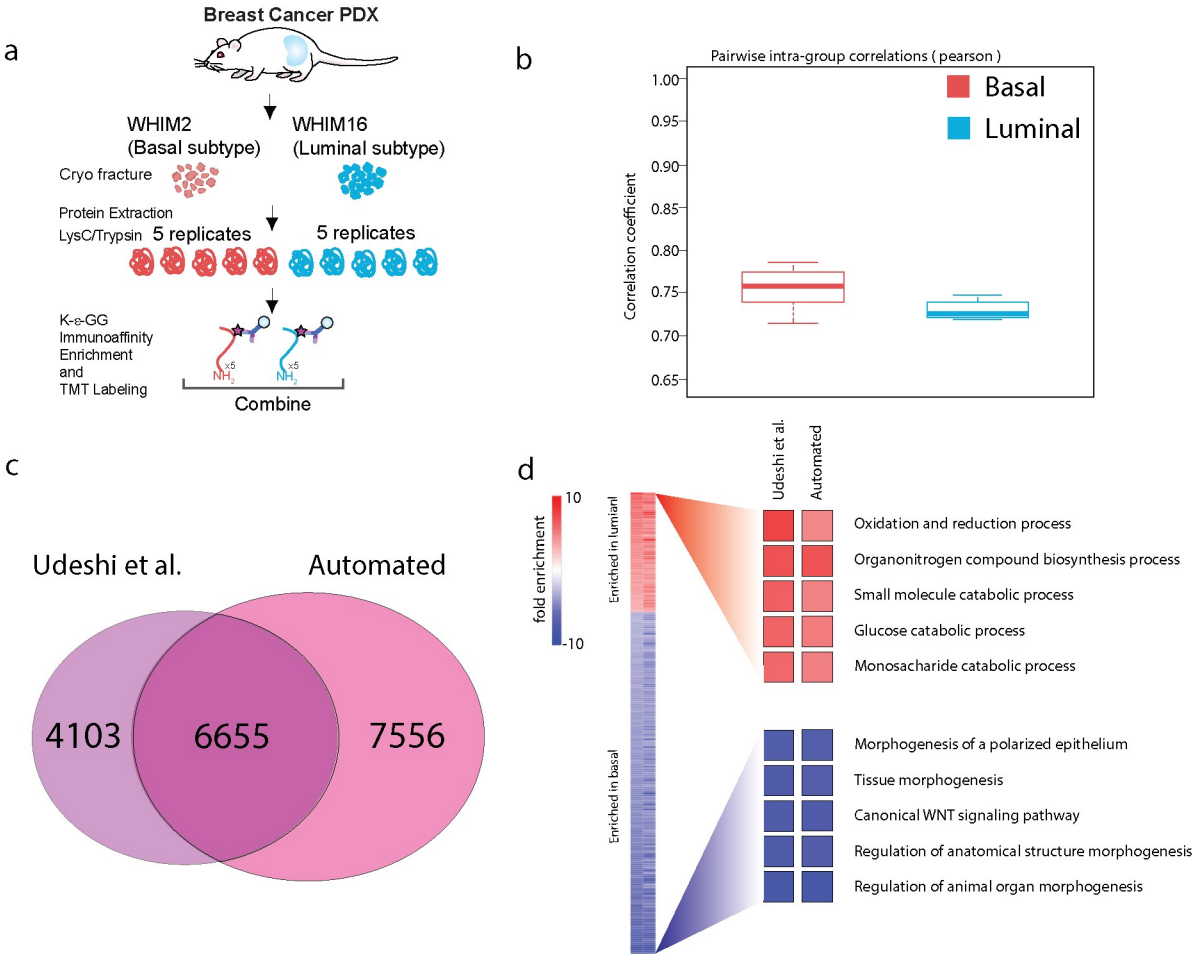

Figure 4

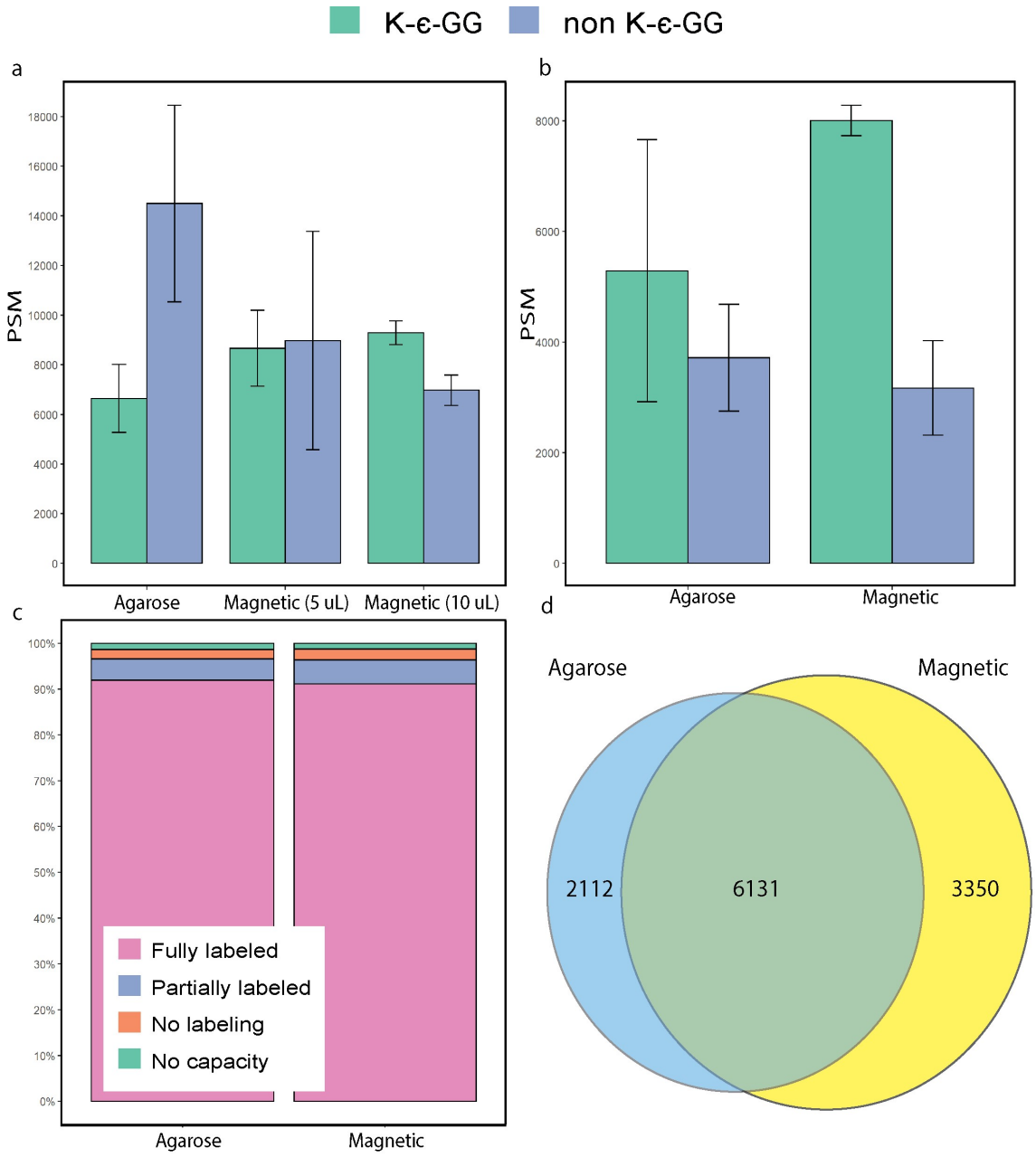

e

	K-ε-GG PSMs	Fully Labeled K-ε-GG PSMs	Partially Labeled K-ε-GG PSMs	Relative Yield of K-ε-GG PSMs
Agarose Beads (label free)	6643	-	-	32%
Magnetic Beads (label free)	8662	-	-	51%
Agarose Beads (labeled with TMT)	5290	91%	5%	57%
Magnetic Beads (labeled with TMT)	8008	91%	5%	72%

Supplemental Figure 1

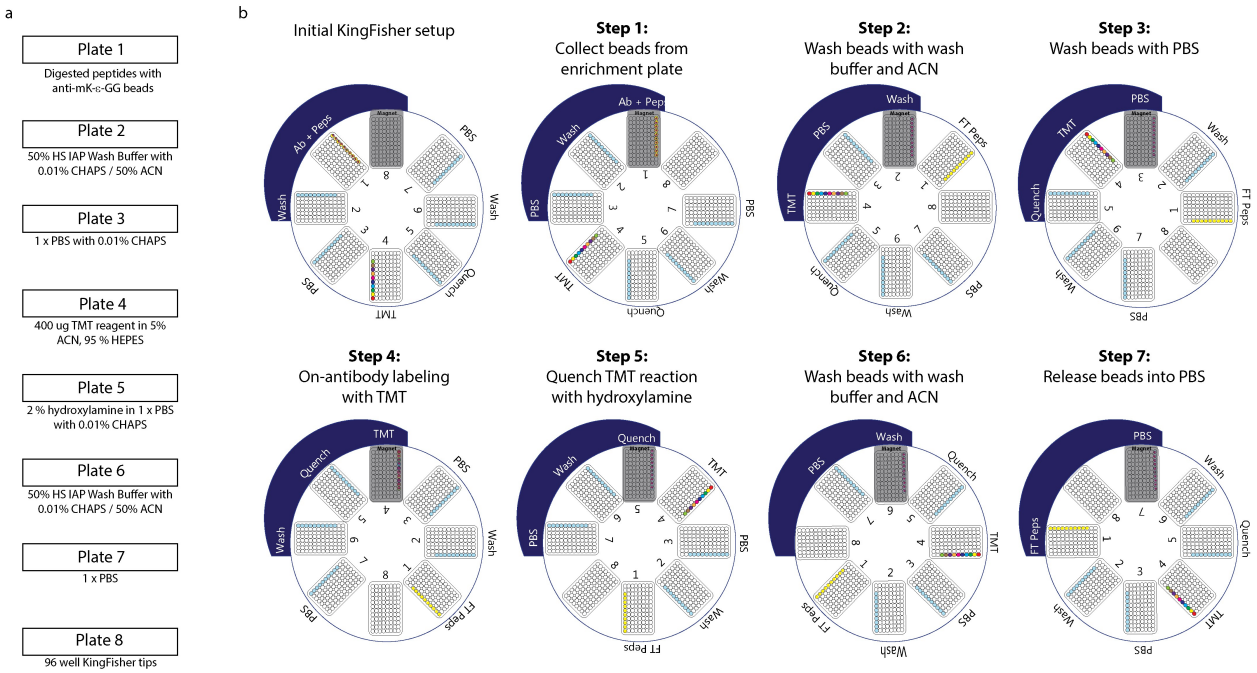

Supplemental Figure 2

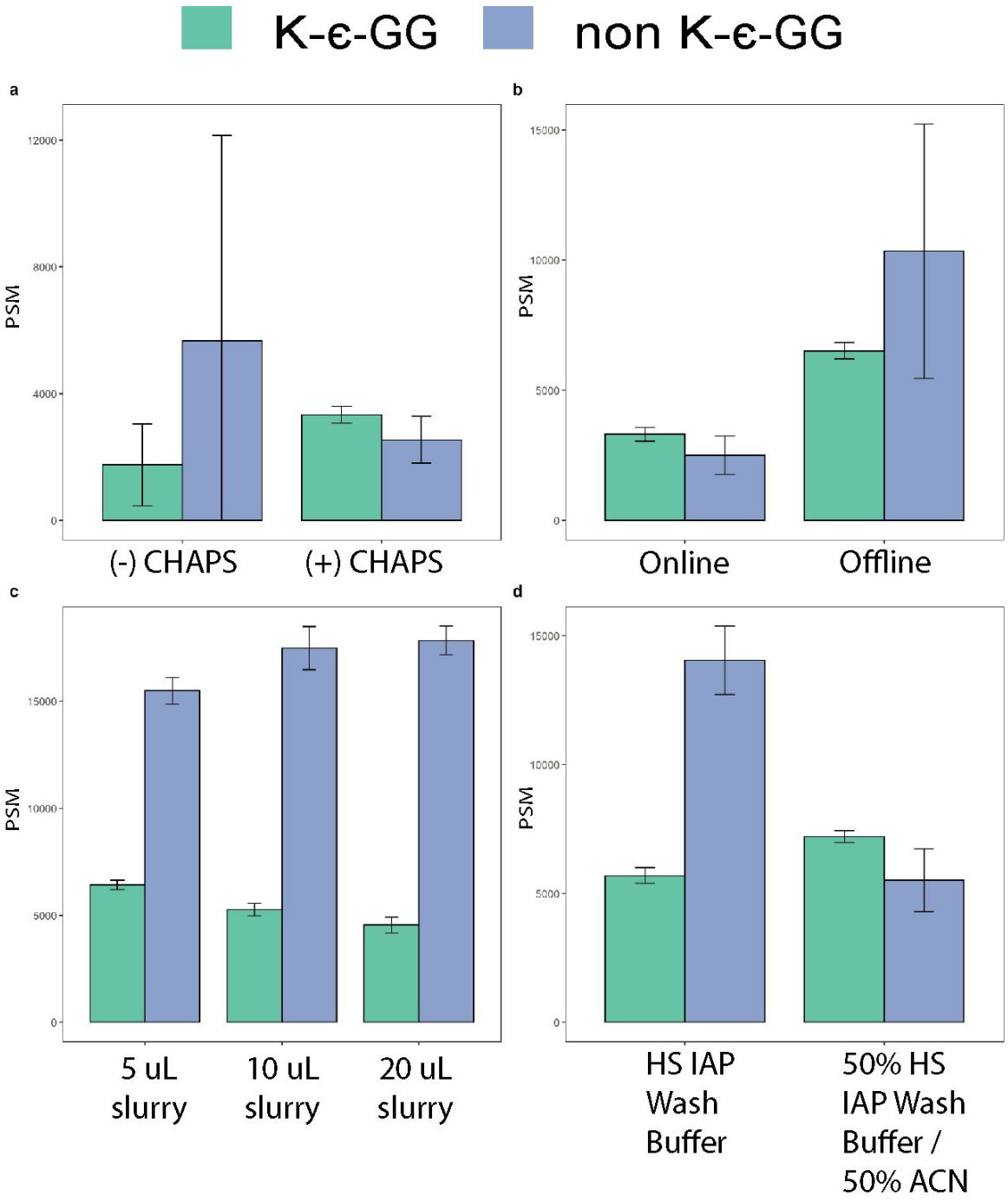

Supplemental Figure 3